The Holocene 11,2 (2001) pp. 161–175

Changes in glacier extent on north Novaya Zemlya in the twentieth century

JaapJan Zeeberg and Steven L. Forman

(Department of Earth and Environmental Sciences (M/C 186), University of Illinois at Chicago, 845 W Taylor Street, Chicago, Illinois 60607–7059, USA)

Received 4 February 2000; revised manuscript accepted 4 April 2000

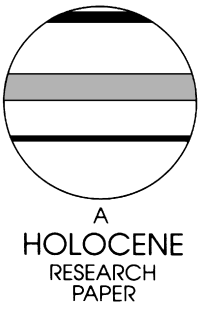

Abstract: Glacier retreat on north Novaya Zemlya for the past century was documented by registering glacier terminus positions from expedition and topographic maps and remotely sensed images. Recession of tidewater calving glaciers on north Novaya Zemlya in the first half of the twentieth century was relatively rapid (>300 m yr^{-1}), consistent with post-'Little Ice Age' warming documented by a 122-year instrumental record from Malye Karmakuly. The glaciers completed 75 to 100% of the net twentieth-century retreat by 1952. Between 1964 and 1993 half of the studied glaciers were stable; the remainder retreated modest distances of <2.5 km. This stability coincides with decreasing average temperatures, especially during the winter, which is counter to model prediction. There is a statistically significant covariance of unfiltered winter and summer temperatures from Novaya Zemlya and a smoothed 88-year record of SSTs in the southern Barents Sea ($r > 0.75$). Elevated SST in the Barents Sea appear to reflect increased advection of warm North Atlantic water associated with a positive North Atlantic Oscillation index (NAO). Winter temperatures are periodically correlated with the NAO ($r = 0.75$ to 0.9) reflecting repeated penetration of Atlantic cyclones into the Arctic. During the twentieth century, an overall positive glacier mass balance trend at Novaya Zemlya is associated with a positive phase of the NAO, elevated southern Barents Sea SST, and a concomitant increase of winter precipitation. Strong NAOs enhance winter precipitation and (3–5 yr delayed) summer temperatures on Novaya Zemlya and have a variable effect on Novaya Zemlya glaciers.

Key words: glaciers, Arctic climate, Novaya Zemlya, 'Little Ice Age', North Atlantic Oscillation.

Introduction

The transition from 'Little Ice Age' cooling to twentieth-century warming is associated with negative mass balances and retreat of glaciers during the past century (cf. Dowdeswell *et al.*, 1997). There are few instrumental records from the Arctic that document the climate change during this transition (e.g., Grove, 1988; Bradley and Jones, 1993). Tree-ring data from the northern tree-line of Scandinavia and the northern Urals, and historical data from western Russia, show that a warm episode commenced in the first two decades of the twentieth century (Bradley and Jones, 1993; Briffa *et al.*, 1995). Glacier retreat on Svalbard is related to a rise of 2–3°C in summer air temperatures since 1912 (Spangler and Jenne, 1990; Dowdeswell *et al.*, 1997; Svendsen and Mangerud, 1997). Glaciers on Svalbard expanded 10+ km beyond present limits during the 'Little Ice Age', *sensu lato* at *c.* 500 to 70 years ago (Baranowski, 1977; André, 1986; Grove, 1988; Werner, 1990; Bennett *et al.*, 1999). Maximum 'Little Ice Age' expansion of glaciers in southern Norway is constrained by ^{14}C dating of buried organics and lichenometric dating to the mid-eighteenth century. This advance is probably associated with a southward displacement of the oceanic polar front and atmospheric storm tracks (Matthews, 1991). Thus, twentieth-century glacier retreat in Norway reflects not only increased summer temperatures but also a decreased frequency of cyclonic depressions and decreased winter precipitation.

Over the past 30–40 years, 83% of the Arctic glaciers have experienced predominately negative net surface mass balances (Dowdeswell *et al.*, 1997). However, maritime and more inland glaciers in Norway, Sweden and Iceland, retreating since the 1920s, are now accumulating mass (Nesje *et al.*, 1995; Caseldine and Stötter, 1993; Pohjola and Rogers, 1997). The largest glaciers at the Norwegian coast have advanced 400+ m since the late 1980s as a result of increased winter mass balances (Nesje *et al.*, 1995; Winkler and Nesje, 1999). Positive mass balances in Scandinavia are related to increased storm activity coincident with a high index of the North Atlantic Oscillation (NAO) in winters post-1980 (Hurrell, 1995; Pohjola and Rogers, 1997). Svalbard, by comparison, is seldom traversed by Atlantic cyclones during the accumulation season (Pohjola and Rogers, 1997), but in some years the storm tracks do extend into the Barents Sea and cyclones may eventually reach Novaya Zemlya (Rogers and Mosley-Thompson, 1995).

This study analyses changes in glacier terminus position on north Novaya Zemlya in the past century and provides new insight on the variable control of precipitation and temperature on glacier position, and potential teleconnections with the North Atlantic region. The earliest glaciological observations on Novaya Zemlya

0959-6836(01)HL444RP

were conducted between 1907 and 1912 by Rusanov (1910; 1921; Lavrov, 1932; Barr, 1974). These observations, together with a map of the northwest coast and tidewater outlet glaciers produced by Georgy Sedov in 1913, were used to assess changes in glacier extent by Chizov *et al.* (1968) and Koryakin (1986; 1988; 1997). The time-series is expanded with remote sensing imagery from 1964 and 1993 and incidental historical observations from 1871, documenting glacier retreat on north Novaya Zemlya over 122 years. The maximum extent of some glaciers in this study is constrained by radiocarbon dates and field observations obtained in 1992, 1995 (Forman *et al.*, 1999) and in August-September 1998. The timing of post-'Little Ice Age' glacier retreat on Novaya Zemlya and potential controls of re-advance are analysed using temperature and precipitation data since 1876 from the Malye Karmakuly weather station (Figure 1). A mass balance time-series on the Shokal'ski Glacier from 1933 to 1969, one of the longest in the Arctic, is concurrent with meteorological observations at the adjacent station Russkaya Gavan' (Chizov *et al.*, 1968; Mikhaliov and Chizov, 1970; Koryakin, 1988). Thus, a quantitative assessment is provided of the effects of temperature and precipitation on glacier mass balance on Novaya Zemlya for the past *c.* 70 years.

Climatology of Novaya Zemlya

Lateral variation of temperature and precipitation

The climate of Novaya Zemlya is influenced by the advection of warm North Atlantic-derived water (water depth between 75 and 250 m) into the Barents Sea (Loeng, 1991; Pfirman *et al.*, 1994). Novaya Zemlya with an average altitude of ~1000 m a.s.l. provides an orographic barrier for the eastward penetration of Atlantic cyclonic systems. The influence of North Atlantic input into the Barents Sea is reflected in the temperatures and precipitation recorded at coastal weather stations Malye Karmakuly (72° 22′N), Russkaya Gavan' (76° 11′N), and Cape Zhelaniya (76° 57′N). The respective mean annual temperature and precipitation for 1955 to 1998 decrease northward, from –5.4°C and 396 mm at Malye Karmakulye (cf. Matzko, 1993) to –8.4°C and 329 mm at Russkaya Gavan', and to –10.3°C and 283 mm at Cape Zhelaniya (Table 1; Figure 1). Temperatures in March at Cape Vychodnoi on the Kara Sea coast are 2°C colder (–18°C) than at Russkaya Gavan', but summer temperatures are similar (Chizov *et al.*, 1968). These colder winter temperatures on the Kara Sea coast reflect mostly permanent sea ice and the dominance of Arctic water.

Temperature and precipitation at Novaya Zemlya show substantial lateral variation and also change as a result of the mountainous topography, with ice sheet elevations up to 1173 m. Due to orographic condensation, the effective precipitation was measured to increase at the Shokal'ski Glacier with 60 to 70 mm per 100 m altitude (Chizov *et al.*, 1968). Total annual precipitation at the ice divide (760 m a.s.l.) amounts to 800 mm, as compared to 329 mm received at sea level. Temperatures decrease by 0.7 to 0.5°C per 100 m altitude (Chizov *et al.*, 1968; Kondrat'eva, 1978), consistent with the saturated adiabatic lapse rate (~0.6°/100 m; cf. Barry and Chorley, 1982).

Temporal variability

The instrumental record of precipitation, temperature and air pressure at Malye Karmakuly, Novaya Zemlya, is one of the longest continuous meteorological time-series in the Arctic, spanning more than a century (Figure 2). There is a noticeable increase in temperature at Malye Karmakuly between *c.* 1920 and *c.* 1961, when summer and winter temperatures were predominately above average. Lower temperatures are frequent since *c.* 1961. Averaged over the period 1962–1997, summer and winter temperatures are respectively 0.8°C (summer) and 2.2°C (winter) higher than between 1876 and 1919 (Table 1). Russkaya Gavan' and Cape Zhelaniya document falling temperatures between 1931 and 1996

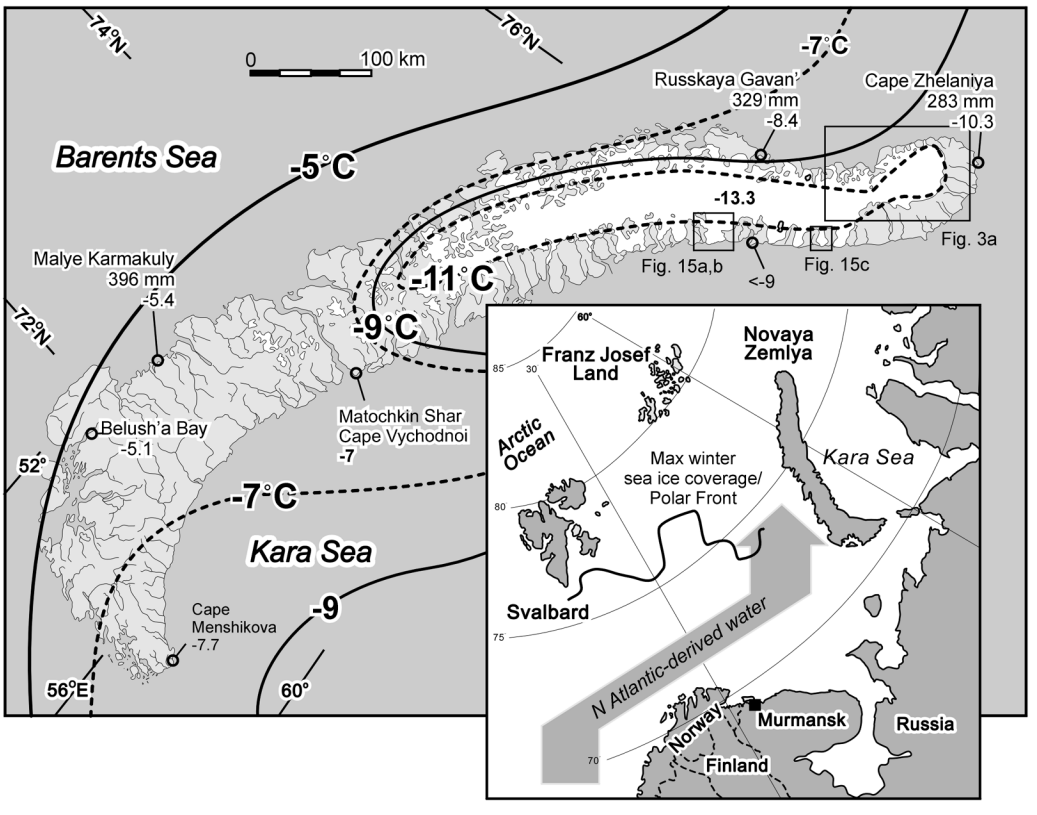

Figure 1 Inferred isotherms for Novaya Zemlya. Average annual temperatures and precipitation for Malye Karmakuly, Russkaya Gavan', and Cape Zhelaniya are calculated over the period 1955–1998 from data provided by the World Data Center-B. Additional temperature records are from Chizov *et al.* (1968) and Kondrat'eva (1978). Inset shows advection of North Atlantic-derived water and maximum sea-ice coverage (Loeng, 1991).

Table 1 Average winter (Tw) and summer (Ts) air temperature (°C ± 0.1) and winter (Pw) and annual (Pa) precipitation (mm) averages for Novaya Zemlya

	Malye Karmakuly[a]				Russkaya Gavan'[b]				Cape Zhelaniya[c]			
	Tw	Ts	Pw	Pa	Tw	Ts	Pw	Pa	Tw	Ts	Pw	Pa
1834–1835	–18.1*	4.7*										
1876–1919	–16.2	5.7			–19.6#	2.9#						
1920–1961	–12.6	6.9			–14.9	3.9			–17.8	2.3		
1962–1997	–14.0	6.5	30	396	–17.4	3.6	27	329	–20.6	1.8	22	283

[a]Malye Karmakuly 72° 22′N, 52° 42′E; 1876 to 1998.
[b]Russkaya Gavan' 76° 11′N, 62° 35′E; 1933 to 1992.
[c]Cape Zhelaniya 76° 57′N, 68° 33′E; 1931 to 1996.
Winter: December through March; summer: July and August; precipitation averaged since 1955. Full time-series are presented in Figures 2 and 17.
*Data for West Matochkin Shar (73° 17′N, 54°E) collected by Von Baer 1834–1835 (Chizov *et al.*, 1968).
#Data for Foki Bay (76° 00′N 60° 00′°E) collected between 1896 and 1925 (Chizov *et al.*, 1968).

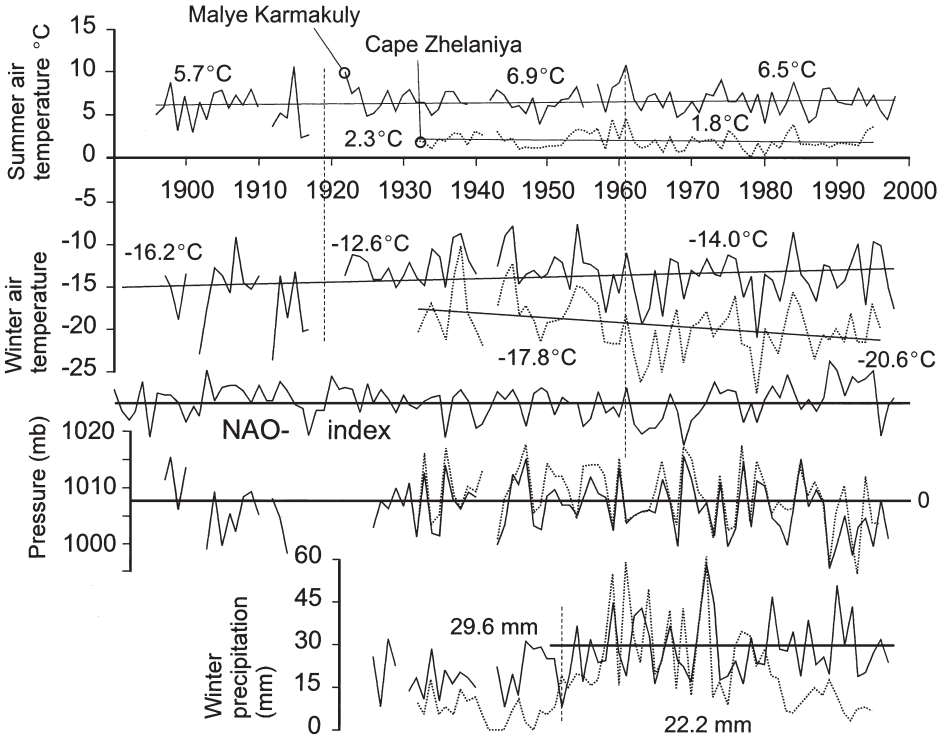

Figure 2 Averaged summer (July–August) and winter (December–March) air temperatures, air pressure, and winter precipitation for Malye Karmakuly (1890–1998) and Cape Zhelanya (1932–1996, dotted lines), compared to the NAO index. The NAO index was taken from http://www.cgd.ucar.edu/cas/climind/nao_winter.html.

(Figures 2 and 17). An expedition lead by Karl von Baer, arriving in the summer of 1834, spent a year in west Matochkin Shar and recorded summer temperatures 1.8°C ± 0.1 lower than today (Table 1). Twentieth-century warming is consistent with other Arctic regions (cf. Warren and Glasser, 1992; Bradley and Jones, 1993; Overpeck *et al.*, 1997).

The precipitation records show a large seasonal and interannual variation, related to shifting atmospheric circulation patterns. Peak precipitation in August coincides with an increasingly dominant westerly airflow and low surface pressure (Chizov *et al.*, 1968). The driest month is April, when air pressure generally rises and easterly or meridional circulation predominates. Mean annual precipitation at Cape Zhelaniya fluctuates between 121 mm (1992) and 512 mm (1964); at Malye Karmakuly from 260 mm (1985) to 565 mm (1990). This variability is related possibly to the interannual fluctuation of sea-surface temperatures in the North Atlantic Ocean and concurrent development of cyclonic disturbances.

Atmosphere/ocean linkages between Novaya Zemlya and the North Atlantic region

The North Atlantic Oscillation (NAO) represents an alternating, interannual polarization of sea-level pressure in the North Atlantic; a regional manifestation of the hemisphere-scale Arctic Oscillation (Hurrell, 1995; Shindell *et al.*, 1999). Both oscillations are related to deepening of the polar vortex (Thompson and Wallace, 1998). A positive NAO represents below-normal sea-level pressure in high latitudes and above-normal sea-level pressure in mid-latitudes (Hurrell, 1995). The expansion of the Azores High increases the poleward pressure gradient over the North Atlantic and, hence, the strength of westerly flow. A large Azores High furthermore shifts the mean pathway of surface flow to northern Europe. A positive NAO reflects an increase of surface evaporation and atmospheric heating, particularly during winter, and on average a 13% intensification of the stormtrack (Rodwell *et al.*, 1999). Enhanced westerlies and deepening of cyclones are associated with positive air-temperature anomalies from northern

Europe (Hurrell, 1995) to central Siberia (Rogers and Mosely-Thompson, 1995; Livingstone, 1999).

The pressure differences between mean sea-level pressure for the 30 coldest and the 30 warmest winter months since 1950 in Arctic Siberia reach maxima (16 mb) over Novaya Zemlya (Rogers and Mosely-Thompson, 1995). These pressure changes are associated with the passage of Atlantic cyclones, which are persistently intense when the NAO remains locked in a positive phase for consecutive years. Prolonged positive phases of the wintertime NAO occurred between 1902 and 1914, 1919 and 1927, 1943 and 1951, and since 1980 (Figure 2). During those periods, North Atlantic air masses reach deep into the Eurasian Arctic, resulting in elevated precipitation at Novaya Zemlya. In periods with a prolonged negative NAO-index, for instance between 1954 and 1971, cyclones are comparatively weak and confined to areas near Labrador and southern Greenland (Rogers and Mosely-Thompson, 1995).

Assessment of glacier extent and ELA with maps and remote sensing images

Glacier observation

Glacier retreat on north Novaya Zemlya for the past century was documented by registering glacier terminal positions from early twentieth-century expedition maps, topographic maps and remotely sensed images. The datum for assessing glacier margin position change is the present glacier margin position, observed on a satellite image of January 1993. Glacier extent prior to 1913, the first year of observation for most glaciers in this study, is inferred from the extent of moraines (Figure 3). These are minimum estimates of the maximum glacier extent. The oldest observations are for the Bunge and Petersen glaciers, which in 1871 were advanced beyond fjord confines (Chizov *et al.*, 1968; Petermann, 1872). Glacier margin positions in 1913 are well indicated by a coastline map of northwest Novaya Zemlya produced by Georgy Sedov (Chizov *et al.*, 1968; Barr, 1973). Glacier retreat between 1913 and 1933 was documented during a glaciological expedition to Russkaya Gavan' in 1933 (Chizov *et al.*, 1968; Jermolaev, 1934). Glacier margin positions in 1952 are fixed by the first topographic map of Novaya Zemlya. Map production was assisted by air photos acquired on 25 July 1952 and included altimetry of the ice caps and individual landforms by land-surveyors. The topographic map at a 1:200 000 scale was updated in 1971, but retains glacier positions of 1952.

Novaya Zemlya was targeted during the 1960s by the first generation of US spy-satellites (Keyhole-4A; Table 2) providing 'intelligence photography' which was declassified for public use in 1996 (*Corona*-series, USGS). The imagery consists of panchromatic photographic film attaining a maximum, blow-up resolution of 3 m. The resulting images are comparable to air photos on scales of ~1:30 000. Because access to air photos and topographic maps of Novaya Zemlya is still restricted for non-Russians, the *Corona*-imagery provides an essential tool for mapping glacier positions and associated moraines. Individual moraine crests are evident on *Corona*-images and clear glacier margin positions (e.g., Figures 4 and 10). An ERS-1 synthetic aperture radar (SAR) image acquired on 26 January 1993 was used to assess glacier position changes and melt properties of the snow pack (C-band; ground resolution ~25 m/pixel). Maps and images were rectified to a common base map by aligning to prominent moraines and distinctive coastal capes. Glacier positions from *Corona*-images (1964) and the SAR-image (1993) were plotted on the 1:200 000 topographic map (1952) and subsequently measured with an accuracy of ±100 to 200 m (1 to 2 mm on the map).

Inferring equilibrium-line altitude from Synthetic Aperture Radar (SAR) images

The late-summer snowline for many glaciers approximates the equilibrium line altitude (ELA) and is well resolved by SAR (Smith *et al.*, 1997; Forster *et al.*, 1997). The dark and light tones of the ice cap on a radar image indicate variations in surface and near-surface snow textures, causing differential backscattering of the radar-signal. The dry winter snow that probably covers the area is quasi-transparent to radar (Rees *et al.*, 1995; Brown *et al.*, 1999). Thus, the ELA is visible in the SAR image of 26 January 1993 as the transition from a radar-bright to a radar-dark zone (Figure 4). This transition is associated with a facies of dry, first-year snow of 1992, appearing bright, and a darkening zone of superimposed ice and firn, which has undergone at last one melt season (cf. Fahnestock *et al.*, 1993; Rees *et al.*, 1995; Brown *et al.*, 1999). The radar-dark surface below the firn line relates to specular returns by smooth glacier ice. The ice facies can be established from ERS-SAR data with an accuracy of 20 to 40 m (Brown *et al.*, 1999). The lower facies was examined in the summer of 1998 on the ice margin near Ivanov Bay. The glacier was mostly snow-free with meltwater channels occurring to at least 330 m a.s.l. These meltwater channels also can be traced in the *Corona*-satellite image to approximately the same altitude, marking the ablation zone (Figure 4). In the radar image of north Novaya Zemlya the ice margin appears bright by maximum scattering of the radar signal due to normal incidence of the 'painted' surface to the radar beam ('foreslope brightening'). A radar-dark dry snow zone similar to the high interiors of the Greenland and Antarctic ice sheets (Fahnestock *et al.*, 1993) has not been identified at north Novaya Zemlya. Instead, the interior appears bright, indicating the presence of internal scattering elements, e.g. large snow crystals and lenses of refrozen ice in the snowpack (cf. Joughin *et al.*, 1997). The interior ice cap (~550 m a.s.l.) shows darkening in a SAR image of late July 1991, indicating that temperatures have risen above the melting point (L. Smith, personal communication, 1999).

Mass balance measurements

Present mass balance estimates for Novaya Zemlya glaciers are derived from measurements on the Shokal'ski Glacier (Chizov *et al.*, 1968; Mikhaliov and Chizov, 1970), inferences on snow-line positions from air photos taken in July, 1952 (Kotlyakov and Kunakhovitch, no date), and extrapolations with temperature and precipitation data from weather stations (Grosswald and Kotlyakov, 1969). Mass balance measurements at the Shokal'ski Glacier for 1958/59 show an ELA at 700 m, which is consistent with 2°C higher-than-normal summer temperatures (Figure 5). In the 1960s summer temperatures declined and, thus, in 1969 (summer temperature 1.5°C below normal) the ELA was found to be ~500 m, with firn occurring as low as 300 m (Mikhaliov and Chizov, 1970). The average ELA declines south to north on Novaya Zemlya consistent with falling mean annual temperatures. Precipitation arrives with westerlies; therefore the ELA declines toward the Barents Sea (Figure 6). On the cold east side of the island, in the precipitation-shadow of the mountains, the ELA is elevated. However, in the northeast where the topography is ~500 m a.s.l., snow-bearing Atlantic air may penetrate (cf. Dahl and Nesje, 1992; 1996; Aa, 1996). On the SAR-image of the north-eastern glacier margin, the 1992 late-summer ELA is estimated at ~600 m to ~400 m a.s.l. (Figures 3 and 4).

Snowfall, ablation and snow metamorphism have been measured along the Shokal'ski Glacier to 760 m a.s.l. in 1933, 1945, 1950, 1955, 1958, 1959 and 1969 (Chizov *et al.*, 1968). Mikhaliov and Chizov (1970) demonstrated the strong linear relation between summer temperatures and ablation (R^2 = 0.97), and

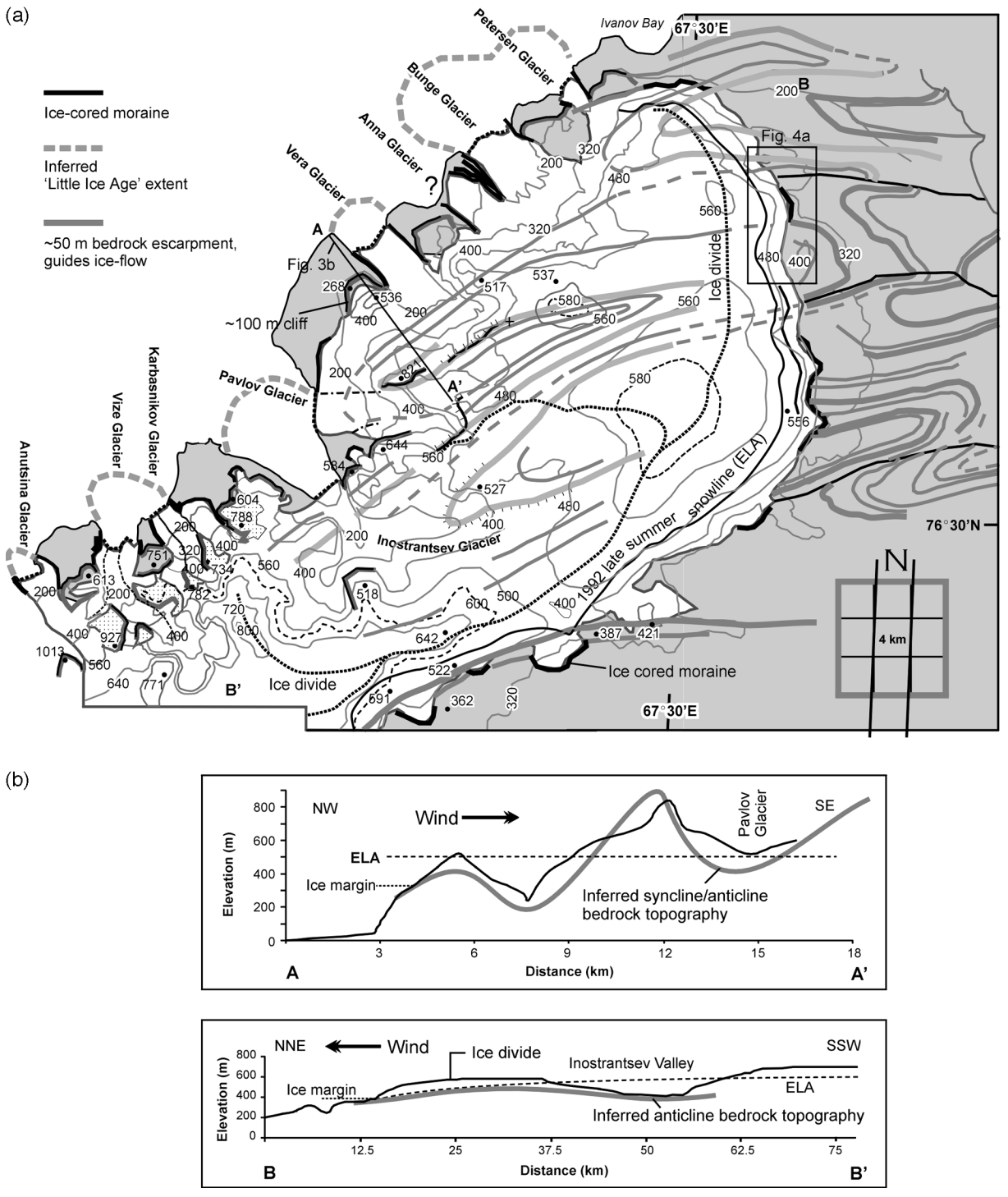

Figure 3 (a) The ice cap and bedrock fold-structures of north Novaya Zemlya (for location see Figure 1). Topography and glacier margin positions from the 1952 topographic map. Ice divides are marked as dotted lines. Grey broken lines represent inferred maximum (nineteenth-century) glacier extent. Bedrock fold-structures, as observed on *Corona*-satellite images, appear to control glacier flow direction. The ELA (from SAR-image; see Figure 4) is indicated as a solid black line. (b) Ice profiles obtained from the 1:200 000 topographic map and anticline/syncline topography inferred from *Corona*-imagery. For the location of profile A–A', see (a). Profile B–B' runs NNE–SSW across the ice cap.

winter temperatures and accumulation ($R^2 = 0.94$; Figure 7). This relation accounts for the elevational difference between the ELA and weather station Russkaya Gavan', which lies within 0.5 km of the glacier terminus. Average summer and winter temperatures of Russkaya Gavan' were applied to the regression formula (Figure 7) to reconstruct a mass balance time-series (Figure 17) for the observation-period of the weather station (1933–1992). The mass balance measurements and meteorological records show that years with a strongly negative mass balance, as for example in 1959, are characterized by the combination of a relatively warm summer and cold winter. The glacier appears to gain mass in years with a relatively cool summer and mild winter.

The inferred mass balance time-series of the Shokal'ski Glacier shows that, in spite of repeated mass gaining and a positive mass balance between *c.* 1945 and 1955, the net mass balance over the period 1930 to 1960 was negative. The average annual loss at the Shokal'ski Glacier was estimated at 57 gr/cm^2 due to melting and ablation (Chizov *et al.*, 1968). Snow accumulation (54 gr/cm^2) nearly compensated ablation, resulting in a small net loss (3 gr/cm^2 per year). At the glacier terminus, the throughput of ice

Table 2 KH-4A (*Corona*) images studied

Image code	Date acquired	Areas studied
DS1030–1053DF007	13 March 1966	75°N to 73° 38′ N (continues 16/3/66)
DS1030–2100DF006	16 March 1966	Guba Mashigina 74° 42′ N to Matochkin Shar
DS1042–2118DF001	24 June 1967	Nordenskiold Bay; Vilkitsky Bay
DS1034–2150DF014	1 July 1966	Ice cap and cirque glaciers, east Matochkin Shar
DS1011–1006DA011	6 October 1964	Russkaya Gavan'
DS1011–1006DF007	6 October 1964	Northern Barents Sea coast of Novaya Zemlya
DS1011–1006DF008	6 October 1964	Cape Zhelanya, central line ice cap
DS1011–1006DF009	6 October 1964	Natalia Bay to Roze Glacier, 2nd and 3rd glacier south thereof
DS1011–1006DA012	6 October 1964	Area north of Russkaya Gavan'
DS1011–1006DA014	6 October 1964	Eastern ice margin

was 150 m/year, which yields a total ice discharge of 16 million m^3 ice $year^{-1}$ (Chizov *et al.*, 1968). Thus, calving was estimated to account for a mass loss of 10 gr/cm^2 $year^{-1}$ on average between 1930 and 1960 (Chizov *et al.*, 1968). This mass loss adds to the 57 gr/cm^2 $year^{-1}$ already accounted for by surface ablation. Hence, over the period 1930–1960 the net mass balance of the Shokal'ski Glacier was –13 gr/cm^2 $year^{-1}$ and strongly controlled by calving.

Changes in glacier extent

Shokal'ski Glacier

The outlet of the Shokal'ski Glacier terminates as a 3 km wide calving front in Russkaya Gavan', a 12 km wide and 100 m deep fjord. A reservoir corrected ^{14}C age of 660 ± 45 yr BP (AA-31370) was obtained on a paired *Astarte borealis*-bivalve retrieved from a transported block of marine sediments in the lateral moraine, presently at a distance of ~500 m from the calving margin. This is a maximum age for the latest Holocene glacier advance in Russkaya Gavan', and calibrates to a calender age of *c.* AD 1300–1400 (Stuiver and Reimer, 1993), consistent with the latest Neoglacial events on Franz Josef Land, either the 'Little Ice Age' advance or just prior to it. Based on the observations of the Sedov-expedition (1913), Jermolaev (1934) estimated 2600 m retreat of the Shokal'ski Glacier between 1913 and 1933 (Chizov *et al.*, 1968). The glacier re-advanced ~300 m between 1933 and 1952. The 1964 *Corona*-image shows additional net retreat of about 400 m compared to the 1952 position. The SAR-image shows that in 1993 the glacier had re-advanced by at least 400 m close to its position in 1952.

Anutsina and Vize Glaciers

The 2.5 km wide Anutsina Glacier, 60 km north of the Shokal'ski Glacier, terminates as a calving margin in the Barents Sea. In 1993 the Anutsina Glacier had receded 3 km from the position of 1913 (Chizov *et al.*, 1968). On the 1964 *Corona*-image moraines (ice-cored?) of presumed 'Little Ice Age'-age curve around the glacier front, suggesting that the first observation (1913) occurred when the glacier was at or near its maximum 'Little Ice Age' extent. The glacier re-advanced about 600 m between 1952 and 1964 and retreated about 800 m by 1993.

The Vize Glacier in 1993 had retreated approximately 8 km from its 1913 position (Figure 10). The majority of the net glacier retreat (7 km) was completed before 1952. The glacier margin position of 1933 was recorded by I.F. Pustovalov (1936; in: Chizov *et al.*, 1968) demonstrating a retreat of 4.6 km between 1913 and 1933. Calving accounts for 2.4 km retreat between 1933 and 1952 (Chizov *et al.*, 1968). Comparison of the glacier margin position on the topographic map and the SAR image reveals a retreat of ~1400 m in the 40 years between 1952 and 1993 (Table 3).

R'ikatseva, Brunova, and Karbasnikov glaciers

Available observations of the R'ikatseva, Brunova and Karbasnikov glaciers indicate stable margins since 1952; there has been <400 m change in margin position in the past 40 years. The R'ikatseva Glacier originates at an ice dome reaching an altitude of 808 m a.s.l., 30 km inland from its ~8 km wide tidewater calving front (Figure 9). The observed glacier position in 1952 is almost 7 km behind the 1913 terminus. Most of the retreat (5 km) occurred between 1913 and 1933. After 1952, the glacier receded another 800 m and since 1964 there is little (<400 m) change in the glacier terminus position. Deltaic sediment accumulation in front of the R'ikatseva Glacier indicates relatively shallow (~10 m) proglacial water depth. The 7 km wide R'ikatseva Glacier sinuously descends, overriding bedrock obstacles before discharging into the Barents Sea. In the 1964 *Corona*-image, the outer reaches of the glacier are inset behind steep-walled (ice-cored) moraines and appear isolated by glacier lowering. There appears to be little change in the glacier terminus since 1964, probably because the ice margin remains pinned on the bedrock obstacle.

The Brunova Glacier occupies the 2 km wide parallel-walled Maka Fjord, south of the Anutsina and Vise Glaciers. The glacier follows the sinuous course of the fjord (Figure 3). In 1913, the glacier was observed at an advanced position at approximately ~5 km beyond the fjord mouth. The bathymetry shows an approximately 30 m high, curved shoal at a water depth of 100 m. This shoal possibly represents a moraine bank, indicating maximum glacier extent during the 'Little Ice Age' (e.g., Hambrey, 1994; Wiles *et al.*, 1995). In 1933, the Brunova Glacier was observed terminating at the fjord mouth. Total retreat of the Brunova Glacier prior to 1952 is ~14 km (Chizov *et al.*, 1968). Calving and retreat increase linearly with water depth (Warren, 1993; Wiles *et al.*, 1995) and the relatively high rate of retreat (100% of net retreat completed by 1952) reflects greater depths inside the fjord (>150 m). The extent of the Brunova Glacier has not varied appreciably (<100 m) since 1952.

The Karbasnikov Glacier immediately north of Vize Glacier is a 3 km wide, ~15 km long glacier which cascades down from the ~700 m high main icefield. This glacier is separated from an unnamed piedmont glacier on its northern side by a lateral moraine (Figure 10). The Karbasnikov Glacier in 1913 extended into the Barents Sea almost 4 km from its present terminus at the coastline. The glacier retreated 3 km between 1913 and 1933 and retreated an additional 800 m by 1952. Post-1952 there is little change (<100 m) in the glacier terminus position.

Inostrantsev, Pavlov and Vera Glaciers

A circular ice cap, with a diameter of 40 to 50 km, exists north of 76° 20′N (Figure 3). This northern ice dome has an asymmetric profile, with a steep southwestern flank and parabolic, land-terminating northeastern side (Figure 3b). The asymmetry reflects ice drainage via six outlet glaciers, of which the 35 km long ice stream of the Inostrantsev Glacier is the most prominent.

The Inostrantsev Glacier is a tidewater glacier discharging into the 14 km wide, 130 m deep Inostrantsev Bay (Figure 11). The Inostrantsev Glacier flows from the 580 m high ice cap by the eastern side of an anticline structure (Figure 3a). Four subglaciers merge to form the 3 km wide Inostrantev Glacier front. The Inostrantsev Glacier retreated 4.4 km between 1913 and 1933, 9 km

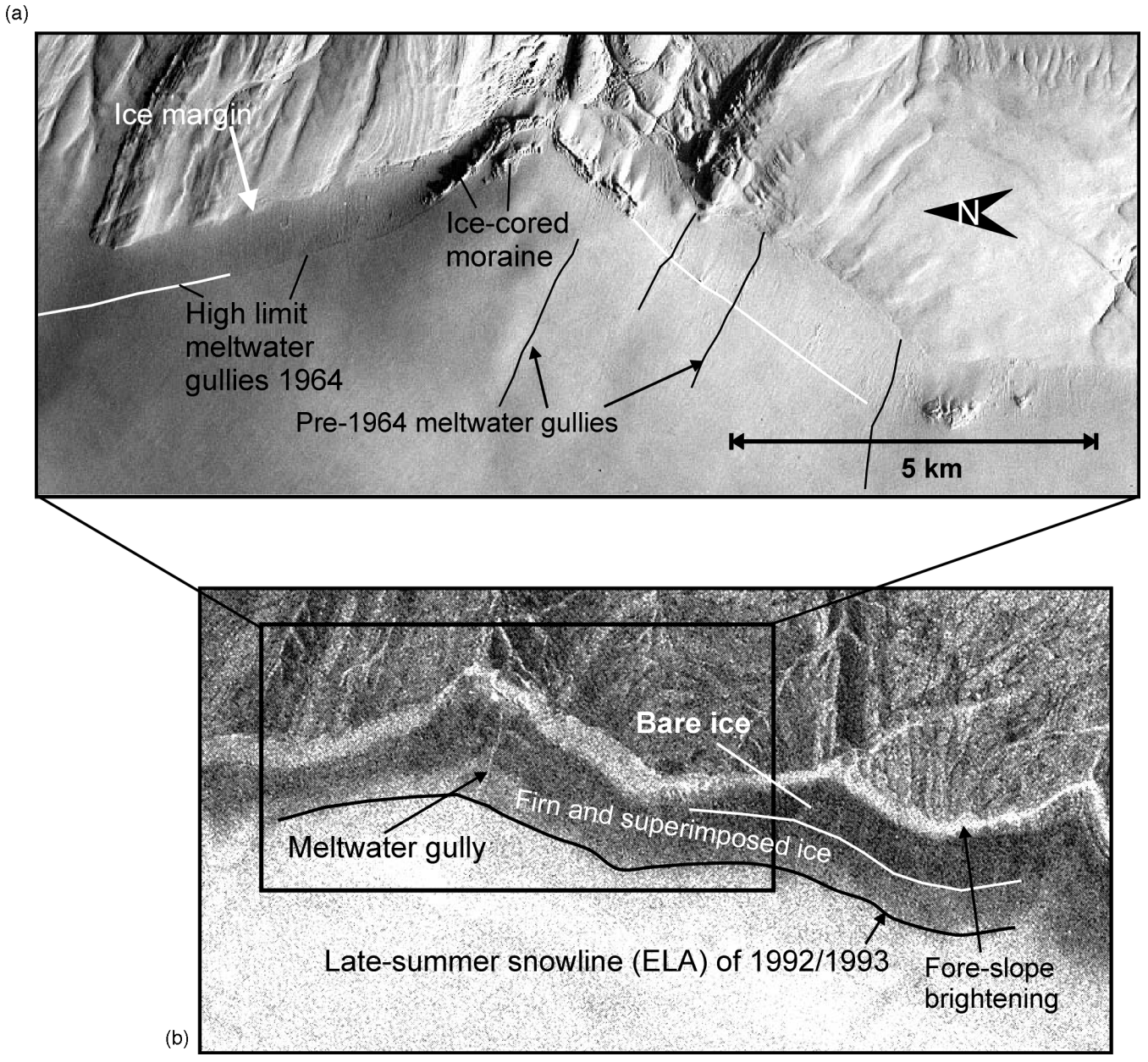

Figure 4 (a) ELA-related features identified on a *Corona*-image of 6 October 1964 (for location see Figure 3a); (b) ERS-SAR image of 26 January 1993.

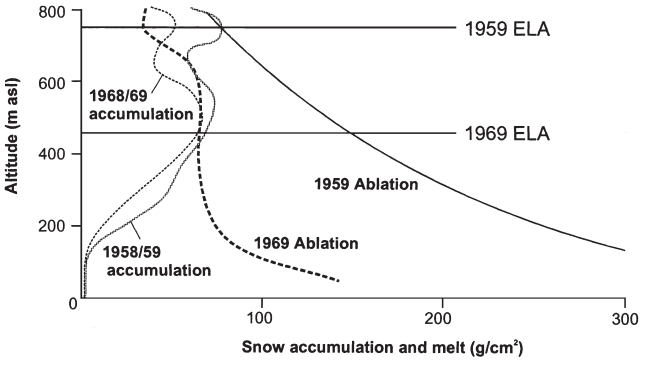

Figure 5 Mass balance measurements at the Shokal'ski Glacier in Russkaya Gavan' for the years 1958–1959 and 1968–1969 (after Mikhaliov and Chizov, 1970).

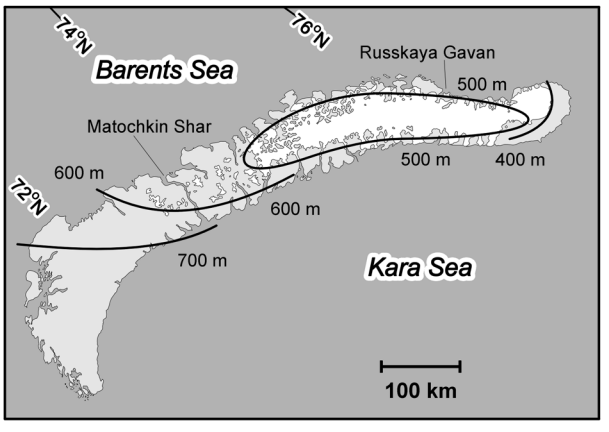

Figure 6 Estimated modern equilibrium line altitudes for Novaya Zemlya, Russia (from Grosswald and Kotlyakov, 1969; Mikhaliov and Chizov, 1970; Kotlyakov and Kunakhovitch, no date; this article).

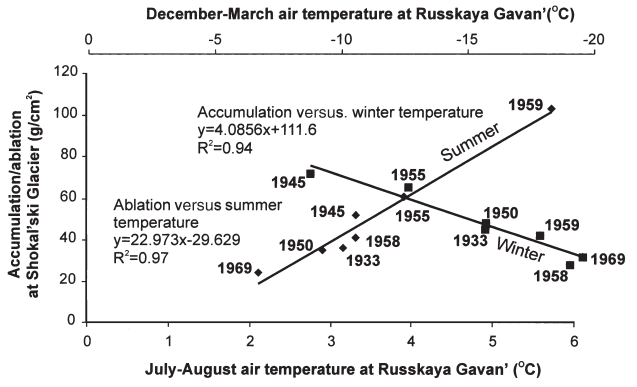

Figure 7 Diagram showing the relation between the mass balanced measured at the Shokal'ski Glacier and summer and winter air temperatures at Russkaya Gavan' (after Mikhaliov and Chizov, 1970); temperature data from the World Data Center-B). The resultant regression is used to calculate the mass balance from the Shokal'ski Glacier between 1933 and 1995 (see Figure 17).

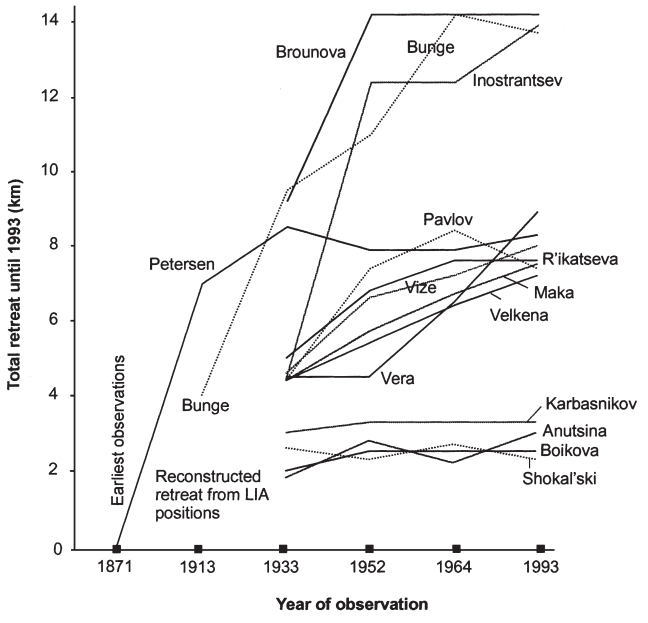

Figure 8 Glacier retreat and advance at north Novaya Zemlya between 1870 and 1993.

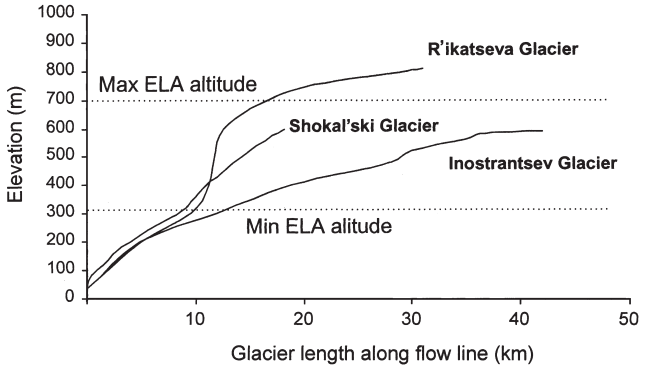

Figure 9 Length and gradient of the Shokal'ski, Ri'katseva and Inostrantsev Glaciers compared with the ELA-range.

between 1933 and 1952, and 1.5 km between 1952 and 1993 (Table 3). The average rate of retreat of 310 m year^{-1} prior to 1952 is comparable to the rate of 350 m year^{-1} found for the Brunova Glacier. The continuous high calving rate of these glaciers (Inostrantsev, Pavlov, Brunova) between 1913 and 1952

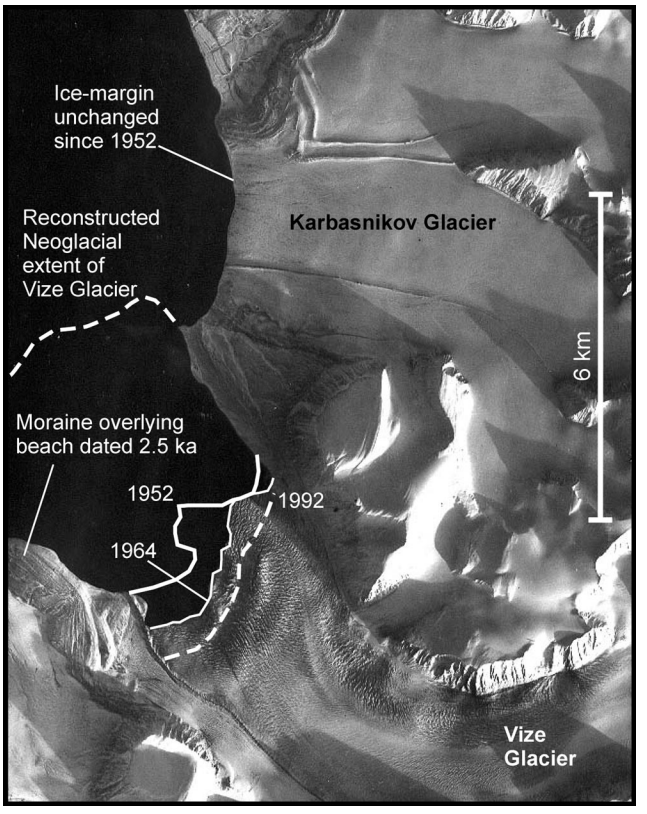

Figure 10 *Corona*-image (1964) showing inferred extent between 1952 and 1993 of the Vize and Karbasnikov glaciers.

probably reflects great water depth in the fjord (>100 m) and exposure to storm-generated swell.

Another glacier discharging into the Inostrantsev Bay is the Pavlov Glacier. The Pavlov Glacier retreated 4.4 km prior to 1933, 3 km between 1933 and 1952, and 1 km between 1952 and 1964 (Table 3). This glacier re-advanced approximately 1 km close to its 1952 position between 1964 and 1993. The SAR-image indicates that the sides of the Pavlov Glacier are abundantly crevassed indicating active glacier movement in 1993 (Figure 11). A fresh 21 m high moraine was found at the front of the Pavlov Glacier in 1998. A paired, juvenile *Chlamys islandica* bivalve collected at 21 m aht from a block of marine silt yielded a post-bomb (younger than 1945) ^{14}C age (AA-31368), indicating a small (<200 m) recent advance. A second, 8 to 15 m high ice-cored moraine can be seen in the *Corona*-image about 1 km away from the ice front (Figure 11). In 1998 this moraine was found to be lichen-free, indicating a recent age. This moraine demarks the maximum (lateral) 'Little Ice Age' extent of the Pavlov Glacier, which is consistent with undisturbed raised beach ridges <1 ka on the outside of the ridge (Forman *et al.*, 1999).

Observations in 1952 indicate that the Vera Glacier was confined to the mouth of the fjord (Figure 12). The glacier margin was probably stabilized at a 30 m high shoal at the entrance of the 100 m deep fjord. The Vera Glacier receded 4 km between 1952 and 1993. At least half (>2 km) of this retreat occurred between 1952 and 1964, thereafter calving slowed from an averaged ~180 m year^{-1} (1952–1964) to ~60 m year^{-1} (1964–1993).

Anna, Bunge and Petersen Glaciers

The Anna, Bunge and Petersen Glaciers are the most northerly outlet glaciers of Novaya Zemlya. In the 1964 *Corona*-imagery the Bunge Glacier flows around a nunatak, forming two outlets (Figure 13). The northern outlet flows around the nunatak and terminates abruptly against the southern outlet, thus limiting its movement. Consequently, the northern outlet appears dark on the SAR image indicating a lack of crevassing (Figure 13b). The

Table 3 Retreat and advance (±100 m) of tidewater calving glaciers at northwest Novaya Zemlya (Arctic Russia) between 1871 and 1993; and percentage of net retreat in 1993

Year	1871	1913	1933	1952[a]	1964[b]	1993[c]	Net	Ref.
Petersen	0	–7000	–1500	+600 (95%)	0	–400	–8300	d, p
Bunge	0	–4000	–5500 (69%)	–1500 (80%)	–3200	+500	–13700	p, e
Vera	0	–	–	–4500 (50%)	–2000	–2400	–8900	c
Pavlov	0	–	–4400 (59%)	–3000 (100%)	–1000	+1000	–7400	p
Inostrantsev	0	–	–4400 (31%)	–8000 (89%)	0	–1500	–13900	p
Karbasnikov	0	–	–3000 (90%)	–300 (100%)	0	0	–3300	p
Vize	0	–	–4600 (57%)	–2000 (82%)	–600	–800	–8000	p
Anutsina	0	–	–1800 (60%)	–1000 (93%)	+600	–800	–3000	p
Brunova	0	–	–9200 (65%)	–5000 (100%)	0	0	–14200	p
Boikova	0	–	–2000 (80%)	–500 (100%)	0	0	–2500	p
Maka	0	–	–4400 (58%)	–1300 (76%)	–1000	–800	–7500	p
Velkena	0	–	–4400 (61%)	–1000 (75%)	–1000	–800	–7200	p
R'ikatseva	0	–	–5000 (66%)	–1800 (89%)	–800	0	–7600	p
Shokal'ski	0	–	–2600	+300	–400	+400	–2300	j

[a]Glacier position change between 1933 and 1952; from Chizov *et al.* (1968).
[b]Topographic map – *Corona*-image.
[c]*Corona*-image – SAR-image.
[d]Petermann, 1872.
[e]Minimum estimate of maximum extent (see text).
[j]Glacier position change between 1913 and 1933; Jermolaev (1934).
[p]Glacier position change between 1913 and 1933; I.F. Pustovalov (1936) in Chizov *et al.* (1968).

Bunge Glacier, similar to the Vera Glacier, retreated in 1952 to within the limits of its relatively shallow (50–70 m) fjord. Ice expansion beyond the fjord would have caused the glacier front to diverge, thereby increasing the calving area and decreasing ice advance (Wiles *et al.*, 1995). The formation of a moraine bank stabilized the glacier terminus at its extended position. The most seaward extent of the Bunge Glacier is indicated by an arcuate shoal, interpreted as a moraine bank, at water depth <30 m. This position is consistent with the extent of the Bunge Glacier observed by the Sedov-expedition in 1913. The glacier receded about 5.5 km between 1913 and 1933, and another 1.5 km until 1952 (Chizov *et al.*, 1968). Subsequently, the glacier receded 3 km between 1952 and 1964, then re-advanced 500 m between 1964 and 1993.

The Petersen outlet is a relatively small glacier, 4 km long and 2 km wide, that drains the 580 m high interior ice dome (Figure 3). Observations in the nineteenth century suggest that Petersen Glacier completed the majority of retreat, about 7 km, prior to 1913 (Petermann, 1872; Chizov *et al.*, 1968). There appears to be little change of the glacier terminus during the twentieth century. Comparison of the 1952 air photo and the 1993 SAR-image indicates glacier advance and retreat <400 m (Figure 14).

Over the past century the land-based Anna Glacier (also: Central Glacier) was not as extensive as neighbouring Bunge and Vera Glaciers. The Anna Glacier in 1952 terminated on land and shows no change in position in the 1964 and 1993 images (Figure 13). The 1964 *Corona*-image shows supraglacial meltwater channels, indicating melting and seasonal lowering of the glacier surface.

Twentieth-century trends in glacier extent

The outlet glaciers on the western side of the northern ice cap retreated between 2+ and 14+ km from positions reached during the 'Little Ice Age' (Figures 3 and 8). However, the land-based northeastern ice margin, extending over a distance of 150 km, varied little (<400 m) between 1952 and 1993 and in places is inset behind 'Little Ice Age' moraines (Figure 4). On the *Corona*-images these moraines have a distinct ridge-and-furrow morphology associated with ice-cored moraines (Østrem, 1964; 1971). The kettled moraine topography observed in the field (Ivanov Bay) furthermore indicates the presence of an ice core. On one occasion the ice core was exposed as a result of slumping near a meltwater stream. The moraines were found to be lichen-free, suggesting recent ('Little Ice Age') emplacement. In the study area, the glacier margin retreated about 300 m from the moraines. The till-covered dead ice zone indicates that recession of the ice margin visible on imagery has occurred through ice surface lowering.

The greatest recession of tidewater calving glaciers on north Novaya Zemlya occurred in the first half of the twentieth century. The apparent retreat rate between 1913 and 1952 is >300 m/year. The estimated average retreat rate post-1952 for Novaya Zemlya glaciers is 50 to 150 m/year. High rates of retreat were probably stimulated by fjord depth and exposure to swell, increasing calving rates. Ten of the 11 glaciers studied by 1952 had completed 75 to 100% of the observed net retreat in 1993 (Table 3; Figure 8). Several outlet glaciers showed no net change in position (Karbasnikov, Brunova, Boikova, Pavlov and Shokal'ski) between 1952 and 1993; others (Petersen, Bunge, Inostrantsev and Velkena) for the same period showed modest retreat of 0.4 to 1.8 km, consistent with slightly negative mass balances. Only the Vera Glacier sustained full retreat since 1952 of 8.9 km, reflecting the dominance of calving.

Controls on the glacier mass balance of Novaya Zemlya

Strength and variability of atmospheric and oceanic controls on Novaya Zemlya climate

Post-'Little Ice Age' glacier retreat at north Novaya Zemlya accelerated in the first or second decade of the twentieth century, and was probably initiated by climate warming, also recorded in other Arctic regions (e.g., Bradley and Jones, 1993; Overpeck *et al.*, 1997). The observed stabilization and recent advance of several tidewater glaciers reflects increased precipitation and/or decreased summer temperatures at north Novaya Zemlya in the second half of the twentieth century. The weather stations at Novaya Zemlya since 1961 document summer temperatures 0.3 to 0.5°C and winter temperatures 2.3 to 2.8°C lower than in the previous period (Figure 2). This is counter to warming of the Eurasian Arctic pre-

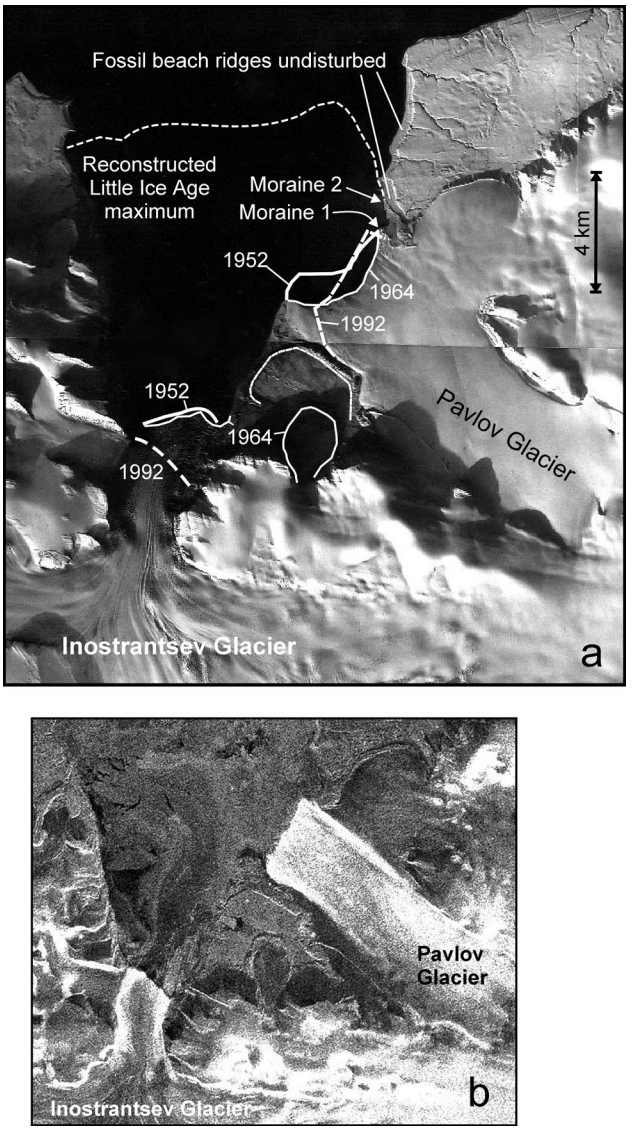

Figure 11 (a) *Corona*-image (1964) showing inferred extent between 1952 and 1993 of the Pavlov and Inostrantsev glaciers; (b) Pavlov and Inostrantsev glaciers on a SAR-image (1993).

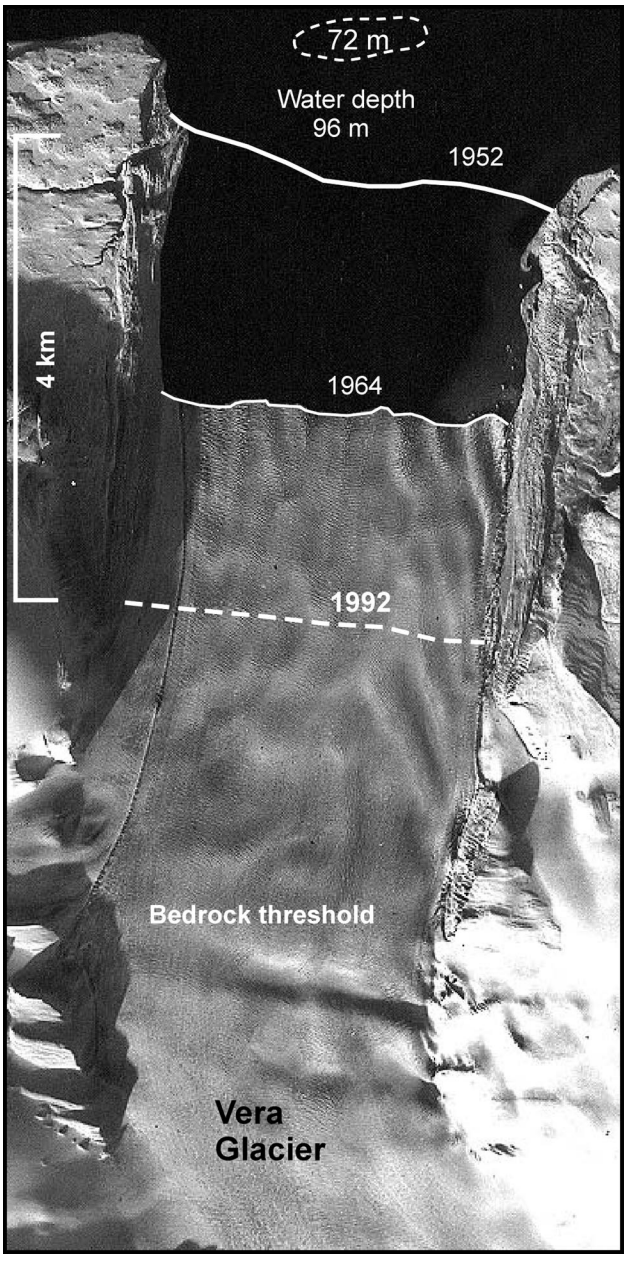

Figure 12 *Corona*-image (1964) showing inferred extent between 1952 and 1993 of the Vera Glacier.

dicted for the twenty-first century by climate models, particularly for the winter season (Cattle and Crossley, 1995; Kattenberg *et al.*, 1995; Overpeck *et al.*, 1997).

There is an apparent periodic covariance of temperature and precipitation on Novaya Zemlya and sea-surface temperature (SST) in the southeastern Barents Sea (Murmansk; Figure 1). To test this covariation, Pearson correlation coefficients (r) were calculated with a seven-year moving average to remove low frequency variability and assess annual to decadal relations. The correlation between a smoothed 88-year record of SST (Loeng, 1991) and unfiltered winter and summer temperatures from Malye Karmakuly and Cape Zhelaniya is significant ($r > 0.75$), except for the periods 1944 to 1953 and 1964 to 1966 (Figure 16A). This lack of correlation is interpreted to represent absence or decline of the oceanic heat source (Figure 17), reflecting decreased advection of North Atlantic water into the Barents Sea (Loeng 1991; Ådlandsvik and Loeng, 1991).

At least 36% of the variability in southern Barents Sea SST is potentially related to the NAO ($r > 0.6$), particularly during the periods 1915–1925; 1938–1946; and in the 1970s to 1990s (Figures 16B and 17). Increasing southern Barents Sea SST are associated with increased speed of the northward-flowing North Atlantic Current and greater net advection into the Barents Sea during a positive NAO (Hurrell, 1995; Loeng, 1991; Ådlandsvik and Loeng, 1991; Kershaw *et al.*, 1999; Rodwell *et al.*, 1999; Marshall *et al.*, 1997). The predominately positive phase of the NAO from *c.* 1920 to 1946 (Figure 17) appears to have initiated the above average temperatures in the southern Barents Sea between 1920 and 1960. There is a significant negative correlation of the NAO and southern Barents Sea SST in the periods 1926–1930 and 1964–1968 ($r = –0.77$). Rising SST during these periods indicate that, despite the declining NAO-index, advection continued.

The passage of North Atlantic cyclones over the Barents and Kara seas, associated with positive phases of the NAO, often elevates winter temperatures and precipitation on Novaya Zemlya. Spectral analysis of unfiltered records of winter temperature and pressure at Malye Karmakuly and Cape Zhelaniya exhibits peaks at 8.5 and 13.6 years, identical to NAO periodicities, indicating a significant relation between these variables. There is a strong negative correlation ($r = –0.6$ to $–0.95$) between the NAO-index and air pressure at Malye Karmakuly due to the nature of the NAO-index, which is positive in winters with anomalously low pressure at high latitudes. In contrast, the fluctuation of air press-

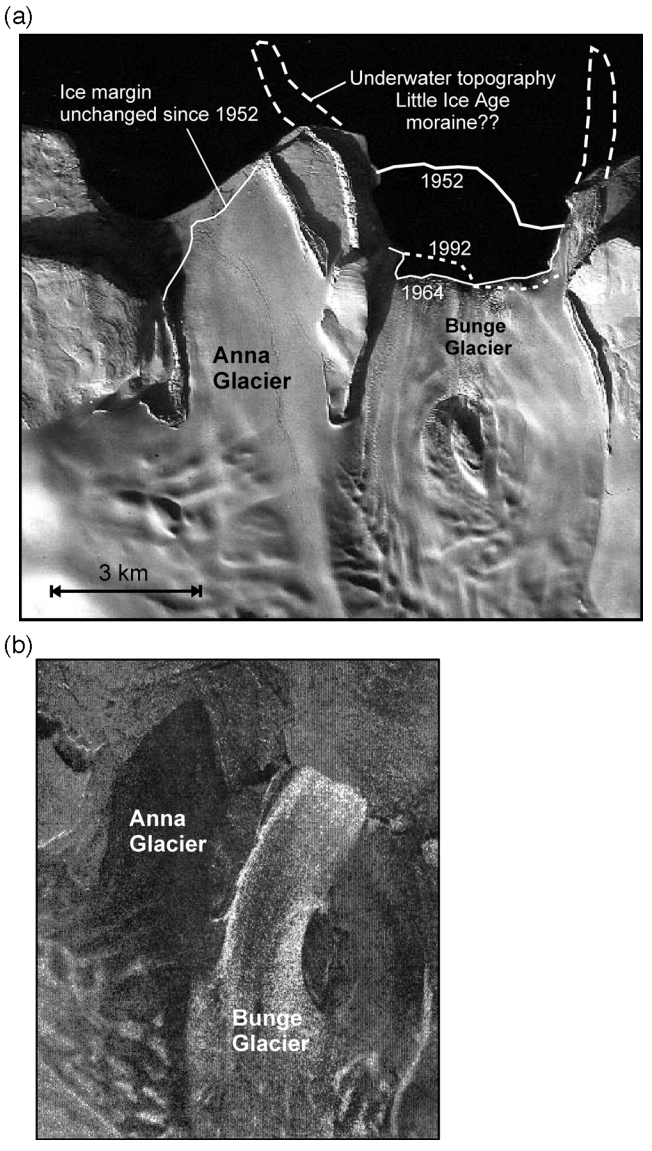

Figure 13 (a) *Corona*-image (1964) showing inferred extent between 1952 and 1993 of the Anna and Bunge glaciers; (b) the Anna and Bunge glaciers on a SAR-image (1993).

ure at Malye Karmakuly is significantly less related to dynamics of the North Atlantic during a prolonged weak and negative phase of the NAO that occurred between 1954 and 1971 (Figure 16C).

Elevated Barents Sea SST and increased penetration of Atlantic cyclones into the Eurasian North are periodically concomitant with a positive or increasing NAO (Figure 16A). Hence, elevated winter and summer temperatures at Malye Karmakulye and Cape Zhelaniya correlate periodically with the NAO (Figure 16D). Unfiltered winter air temperatures covary with the unfiltered (winter) NAO, reflecting the effect of Atlantic-born cyclones on the Barents Sea climate (Rogers and Mosely-Thompson, 1995). Winter temperatures show the strongest positive correlation with the NAO between 1930 and 1944 ($r \sim 0.9$) and between 1974 and 1983 ($r \sim 0.75$). In these periods, rising Barents Sea SST and a concurrent high NAO-index indicate increased influx of North Atlantic Water (Figure 17). There is a delay of three to five years between a strong increase of the NAO and the response of summer air temperatures, probably related to transit time of North Atlantic water to the Barents Sea (Belkin *et al.*, 1998; Kershaw *et al.*, 1999). Hence, summer air temperatures correlate best with the NAO (Figure 16D) during prolonged positive phases, for instance in the periods 1954–1962 ($r = 0.74$ to 0.92) and 1983–1994 ($r = 0.4$ to 0.6).

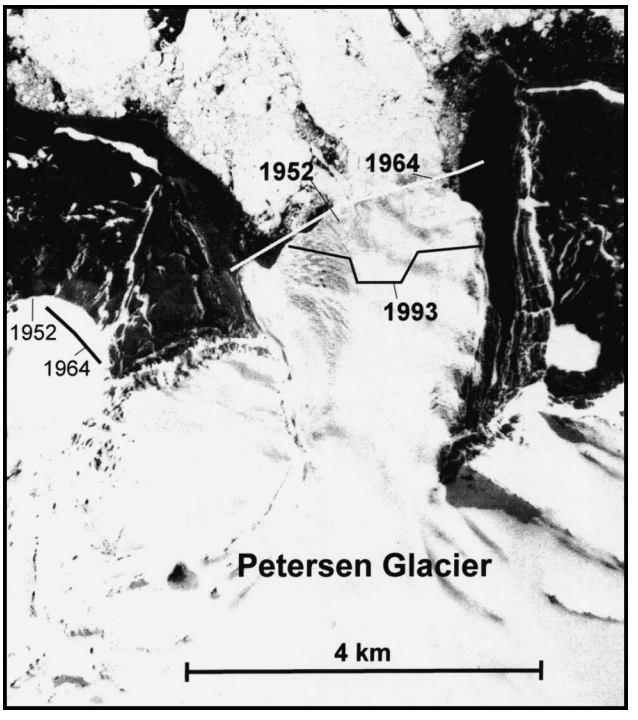

Figure 14 Section from air photo (1952) showing the Petersen Glacier and glacier terminus positions in 1964 and 1993.

Fluctuation of glacier mass balances at Novaya Zemlya and in adjacent regions

Mass balance time series for Svalbard and northern Sweden (50 years) show a close correlation between the summer balance and the annual net balance, implying a common control of summer temperatures (Dowdeswell *et al.*, 1997; Lubinski *et al.*, 1999). Average glacier mass loss at Novaya Zemlya (–0.14 m/yr) is slightly negative, intermediate between Svalbard (–0.55 m/yr) and Franz Josef Land (–0.03 m/yr) (Dowdeswell *et al.*, 1997). The variations in mass balance among the islands in the European Arctic may reflect differences in summer temperature. The average temperature of the warmest month (July) is about +1°C for Franz Josef Land (Lubinski *et al.*, 1999), +3.6°C for Novaya Zemlya (Russkaya Gavan') and +5°C for west Svalbard (Svendsen and Mangerud, 1997). However, time-series of glacier mass balances in north Sweden and the northern Urals correlate with the wintertime North Atlantic Oscillation ($r = 0.6$), reflecting associated increase in winter precipitation (Pohjola and Rogers, 1997). Atlantic storm systems have been persistently strong and glaciers in northern Sweden maintained a positive mass balance during post-1980 winters, coinciding with a prolonged positive phase of the NAO. The correlation between the wintertime NAO-index and glacier mass balances is lower ($r = 0.22$) for glaciers in Svalbard, which, during the accumulation season, usually lies north of the Polar Front and is seldom traversed by Atlantic cyclones (Pohjola and Rogers, 1997).

The mass balance time-series of the Shokal'ski Glacier at Novaya Zemlya (Figure 17) and the IGAN Glacier in the northern ('Polar') Urals (Grosswald and Kotlyakov, 1969) exhibit similar trends, reflecting common atmospheric controls. The mass balance time-series of the IGAN Glacier was entirely negative until 1970 and lies at least 40 g/cm^2 below the time-series for the Shokal'ski Glacier (Figure 17). Although both regions receive between 200 and 250 mm of winter (October–April) precipitation, average summer temperatures at Salekhard in the northern Urals are at least 1°C above those of Malye Karmakuly (Vaganov *et al.*, 1999). In warm years summer temperatures in the northern Urals are >13°C, at least 2°C higher than for Malye Karmakuly in the same years. As a result of the higher summer temperatures, the

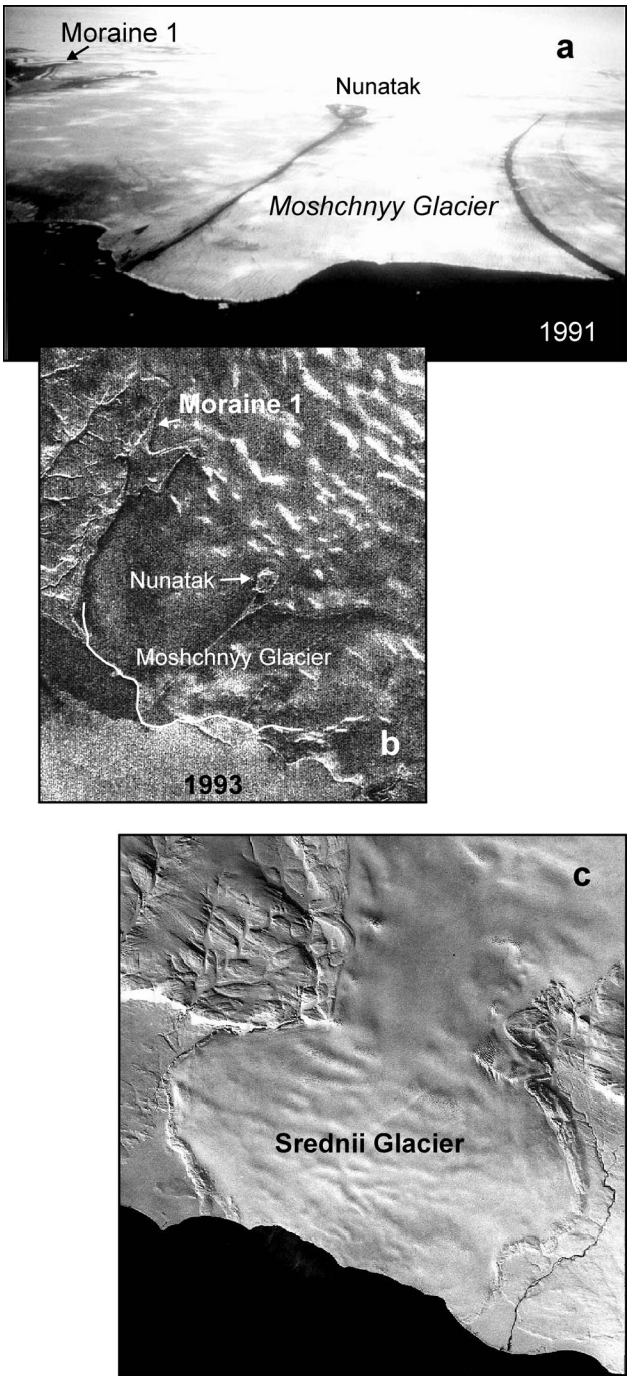

Figure 15 Outlet glaciers of northeast Novaya Zemlya (for location, see Figure 1): (a) the 15 km wide Moshchnyy Glacier (75° 30′N), courtesy Frans Heeres, 25 July 1991; (b) the Moshchnyy Glacier on the ERS-SAR image of 26 January 1993; (c) *Corona*-image showing calving front and lateral moraines of the 10 km wide Srednii Glacier (75° 55′N).

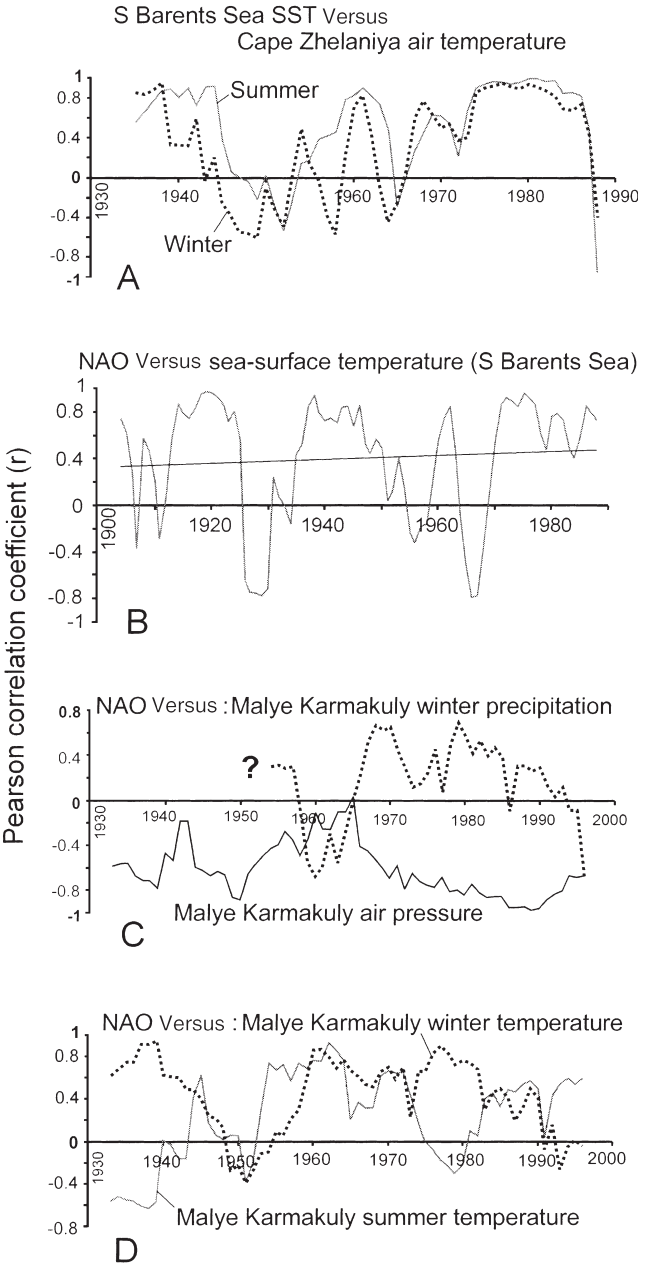

Figure 16 Correlation coefficients (seven-year intervals): (A) Southern Barents Sea SST and Cape Zhelaniya summer and winter air temperature; (B) NAO and southern Barents Sea SST; (C) NAO and Malye Karmakuly winter precipitation and air pressure; (D) NAO and Malye Karmakuly summer and winter air temperature.

equilibrium line altitude is ~1000 m for the IGAN Glacier (Grosswald and Kotlyakov, 1969), compared to about 500 m for the Shokal'ski Glacier. Because the average maximum elevation in the Polar Urals is 1000 m, most valley and cirque glaciers are currently below the ELA. Glaciation on the southern island of Novaya Zemlya is associated with elevations >600 m a.s.l. (Figures 1 and 6).

Analysis of the mass balance measured at the Shokal'ski Glacier in relation to climate is possible for the period post-1953, when Russkaya Gavan' installed instruments that provide a more accurate assessment of winter precipitation by minimizing blowing-out of snow (M. Shaimardanov, World Data Center-B, personal communication). Glacier growth is associated with a positive phase of the NAO, elevated southern Barents Sea SSTs, and a concomitant increase of winter precipitation. However, when summer temperatures rise <1°C above average, ablation compensates for the added precipitation, resulting in a negative (declining) glacier mass balance (Figure 17). Elevated summer temperatures in 1959 and 1961 of 1.8°C and 2.6°C above the 3.9°C average are associated with a negative mass balance of the Shokal'ski Glacier despite anomalous high precipitation in the previous winter (45 mm at Russkaya Gavan'). However, between 1959 and 1966 elevated winter precipitation (up to 20 mm above the 27 mm average), together with the slowing calving rates, arrested the negative mass balance (Figure 17). Glaciers on north Novaya Zemlya are currently poised to either advance or retreat, dependent on the North Atlantic modulated inputs of precipitation and summer warmth (cf. Miller and De Vernal, 1992).

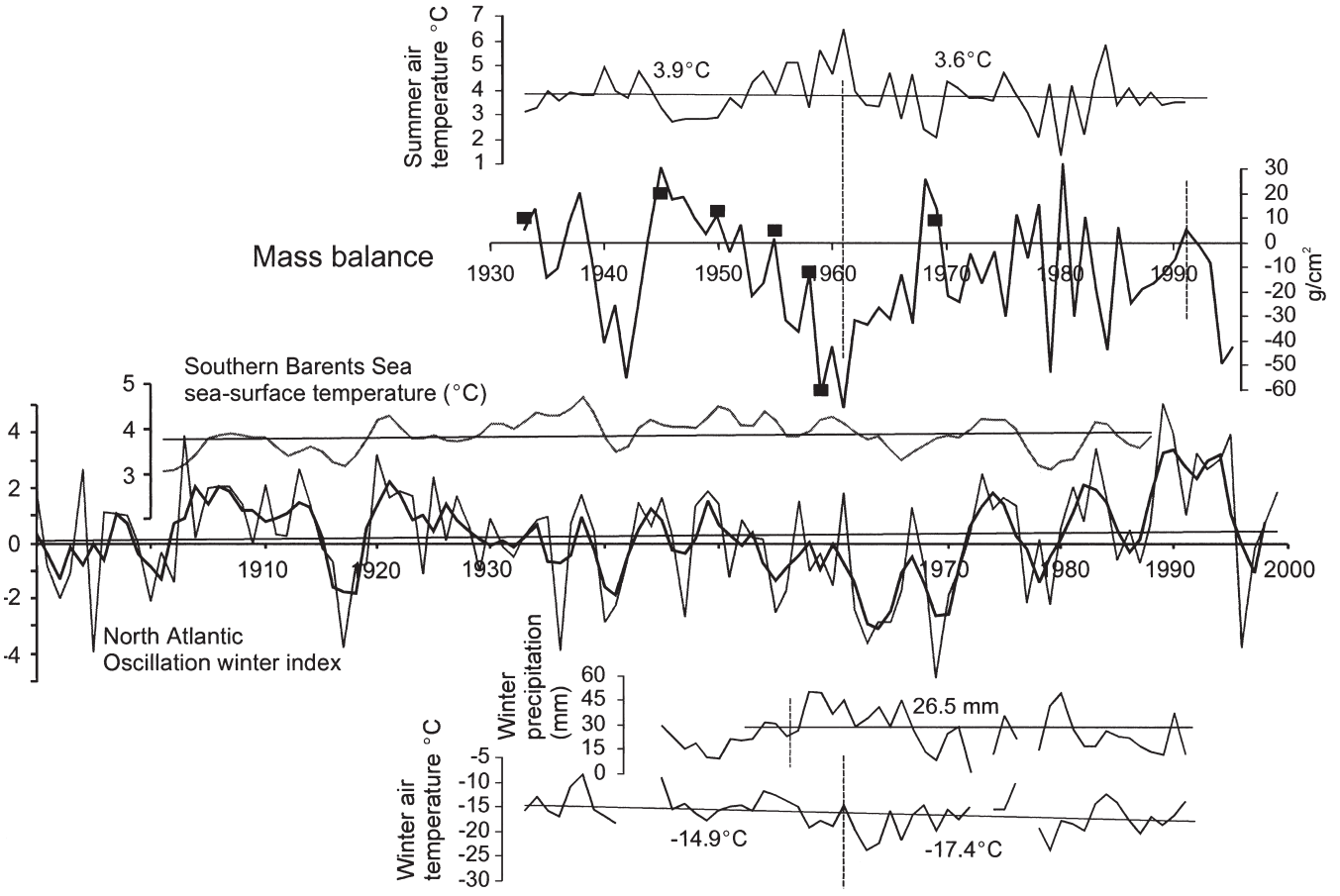

Figure 17 Summer (July–August) and winter (December–March) air temperature and winter precipitation measured at Russkaya Gavan' weather station between 1933 and 1991. Temperature averages are calculated for 1933 to 1961 and 1962 to 1991 (separated by broken lines). Precipitation measurements are accurate since 1956 (indicated by broken line). The mass balance for the Shokal'ski Glacier is calculated by adding the summer and winter balances obtained with the regression formulas shown in Figure 7. Black boxes indicate true measured values. Temperatures for 'missing years' 1942–1944, 1972–1973 and 1991 (broken line) – 1995 were interpolated by comparison with Cape Zhelaniya. The NAO index was taken from http://www.cgd.ucar.edu/cas/climind/nao_winter.html. Bold line is the three-year moving average.

Conclusions

(1) Field-inspected moraines on north Novaya Zemlya were found to be ice-cored and lichen-free, indicating formation connected with the maximum 'Little Ice Age' glacier extent. A ^{14}C age of 660 ± 45 yr BP (AD 1300–1400) was obtained on a paired *Astarte borealis* shell retrieved from a transported block of marine sediments in the lateral moraine of the Shokal'ski Glacier, presently at a distance of ~500 m from the calving margin. This is a maximum age for the latest Holocene glacier advance in Russkaya Gavan'. A paired, juvenile *Chlamys islandica* bivalve collected at 21 m aht from a fresh moraine at the front of the Pavlov Glacier yielded a post-bomb (younger than 1945) ^{14}C age (AA-31368), indicating a small (<200 m) recent advance.

(2) Recession of tidewater calving glaciers on north Novaya Zemlya in the first half of the twentieth century was relatively rapid (>300 m/year). The glaciers completed 75 to 100% of the net twentieth-century retreat by 1952 (Table 3). Between 1964 and 1993 half of the studied glaciers were stable; the remainder retreated modest distances of <2.5 km. Weather stations at Novaya Zemlya since 1961 have documented falling temperatures (Figures 2 and 17), especially during the winter, which is counter to model prediction (Cattle and Crossley, 1995; Kattenberg *et al.*, 1995; Overpeck *et al.*, 1997).

(3) There is a statistically significant covariance of unfiltered winter and summer temperatures from Novaya Zemlya and a smoothed 88-year record of SSTs in the southern Barents Sea ($r > 0.75$). Elevated SST in the Barents Sea appear to reflect increased advection of warm North Atlantic water associated with a positive NAO (Figures 16 and 17). Winter temperatures are periodically correlated with the NAO ($r = 0.75$ to 0.9) reflecting repeated penetration of Atlantic cyclones into the Arctic. There is a delay of three to five years between a strong increase of the NAO-index and the response of summer temperatures, probably related to transit time of North Atlantic water to the Barents Sea. Hence, summer temperatures have the highest correlation with the NAO during prolonged positive phases ($r = 0.6$ to 0.9).

(4) During the twentieth century, a positive glacier mass balance at Novaya Zemlya is associated with a positive phase of the NAO, elevated southern Barents Sea SST, and a concomitant increase of winter precipitation. However, when summer temperatures rise <1°C above average, ablation compensates for the added precipitation, resulting in a negative glacier mass balance.

(5) Strong NAOs enhance winter precipitation and summer temperatures on Novaya Zemlya and have a variable effect on Novaya Zemlya glaciers. Variable control implies a non-linear glacier response of High Arctic glaciers to predicted climate warming. There is a clear need to further monitor glaciers in the High Arctic to determine response to atmospheric and oceanic warming.

Acknowledgements

The cooperation and support of the following persons and institutions is gratefully acknowledged. Fieldwork and data collection

in Russia was executed with D.J. Lubinski and L. Polyak (Ohio State University). Access to Novaya Zemlya was made possible through the efforts of P.V. Boyarsky (Heritage Institute, Moscow) and the crew of R/V *Ivan Petrov*. Meteorological data were provided by M. Shaimardanov of the World Data Center-B for Meteorology (Obninsk, Russia). L.C. Smith (University of California, Los Angeles) assisted with the interpretation of the SAR-image. Russian translation was provided by G. Morozova. This research was supported by National Science Foundation award OPP-9796024.

References

Aa, A.R. 1996: Topographic control of equilibrium-line altitude depression on reconstructed 'Little Ice Age' glaciers, Grovabreen, western Norway. *The Holocene* 6, 82–89.

André, M.F. 1986: Dating slope deposits and estimating rates of rock wall retreat in northwest Spitsbergen by lichenometry. *Geografiska Annaler* 68A, 65–75.

Baranowski, S. 1977: The subpolar glaciers of Spitsbergen seen against the climate of this region. *Acta Universitas Wratislav* 410.

Barr, W. 1973: Sedov's expedition to the North Pole 1912–1914. *Canadian Slavonic Papers* 15, 499–523.

—— 1974: Rusanov, *Gerkules* and the Northern Sea Route. *Canadian Slavonic Papers* 16, 569–611.

Barry, R.G. and **Chorley, R.J.** 1982: *Atmosphere, weather and climate*. London: Methuen, 407 pp.

Belkin, I.M., Levitus, S., Antonov, J. and **Malberg, S.-A.** 1998: 'Great Salinity Anomalies' in the North Atlantic. *Progress in Oceanography* 41, 1–68.

Bennett, M.R., Huddart, D. and **Glasser, N.F.** 1999: Large-scale bedrock displacement by cirque glaciers. *Arctic and Alpine Research* 31, 99–107.

Bradley, R.S. and **Jones, P.D.** 1993: 'Little Ice Age' summer temperature variations: their nature and relevance to recent global warming trends. *The Holocene* 3, 367–76.

Briffa, K.R., Jones, P.D., Schweingruber, F.H., Shiyatov, S.G. and **Cook, E.R.** 1995: Unusual twentieth-century summer warmth in a 1000-year temperature record from Siberia. *Nature* 376, 156–59.

Brown, I.A., Kirkbride, M.P. and **Vaughan, R.A.** 1999: Find the firn line! The suitability of ERS-1 and ERS-2 SAR data for the analysis of glacier facies on Icelandic icecaps. *International Journal of Remote Sensing* 20, 3217–30.

Caseldine, C. and **Stötter, J.** 1993: 'Little Ice Age' glaciation of Tröllaskagi peninsula, northern Iceland: climatic implications for reconstructed equilibrium line altitudes (ELAs). *The Holocene* 3, 357–66.

Cattle, H. and **Crossley, J.** 1995: Modeling Arctic climate change. *Philosophical Transactions of the Royal Society of London* A352, 201–13.

Chizov, O.P., Koryakin, V.S., Davidovich, N.V., Kanevsky, Z.M., Singer, E.M., Bazheva, V.Ya., Bazhev, A.B. and **Khmelevskoy, I.F.** 1968: Glaciation of the Novaya Zemlya. In *Glaciology IX section of IGY Program* 18, 338 pp., Moscow: Nauka (in Russian, with English summary).

Dahl, S.O. and **Nesje, A.** 1992: Paleoclimatic implications based on equilibrium-line altitude depressions of reconstructed Younger Dryas and Holocene cirque glaciers in inner Nordfjord, western Norway. *Palaeogeography, Palaeoclimatology, Palaeoecology* 94, 87–97.

—— 1996: A new approach to calculating Holocene winter precipitation by combining glacier equilibrium-line altitudes and pine-tree limits: a case study from Hardangerjøkulen, central southern Norway. *The Holocene* 6, 381–98.

Dowdeswell, J.A., Hagen, J.O. and nine others 1997: The mass balance of circum-Arctic glaciers and recent climatic change. *Quaternary Research* 48, 1–14.

Fahnestock, M., Bindschadler, R., Kwok, R. and **Jezek, K.** 1993: Greenland ice sheet surface properties and ice dynamics from ERS-1 SAR imagery. *Science* 262, 1530–34.

Forman, S.L., Lubinski, D.J., Zeeberg, J.J. and **Polyak, L.** 1999: Postglacial emergence and Late Quaternary glaciation on northern Novaya Zemlya, Arctic Russia. *Boreas* 28, 133–45.

Forster, R.R., Smith, L.C. and **Isacks, B.L.** 1997: Effects of weather events on X-SAR returns from ice fields: case-study of Hielo Patagonico Sur, South America. *Annals of Glaciology* 24, 367–74.

Grosswald, M.G. and **Kotlyakov, V.M.** 1969: Present-day glaciers in the USSR and some data on their mass balance. *Journal of Glaciology* 8(52), 9–21.

Grove, J.M. 1988: *The Little Ice Age*. London: Methuen.

Hambrey, M.J. 1994: *Glacial environments*. London: UBC Press.

Hurrell, J.W. 1995: Decadal trends in the North Atlantic Oscillation: regional temperatures and precipitation. *Science* 269, 676–79.

Jermolaev, M.M. 1934: Work of the glaciological station on Novaya Zemlya at Russkaya Gavan' (in Russian and English). *Biulleten' Arkticheskogo Instituta* (Leningrad) 4(50–55), 93–98.

Joughin, I., Fahnestock, M., Ekholm, S. and **Kwok, R.** 1997: Balance velocities in the Greenland ice sheet. *Geophysical Research Letters* 24(23), 3045–48.

Kattenberg, A., Giorgi, F., Grassl, G.H., Meehl, J.F.B., Mitchell, J.F.B., Stouffer, R.J., Tokioka, T., Weaver, A.J. and **Wigley, T.M.L.** 1995: Climate models – projections of future climate. In Houghton, J.T., Meira Filho, L.G., Callander, B.A., Harris, N., Kattenberg, A. and Maskell, K., editors, *Climate change 1995*, Cambridge: University Press, 289–350.

Kershaw, P.J., McCubbin, D. and **Leonard, K.S.** 1999: Continuing contamination of north Atlantic and Arctic waters by Sellafield radionuclides. *Science of the Total Environment* 237/238, 119–32.

Kondrat'eva, K.A. 1978: Glacial thicknesses and cryolithozones of Novaya Zemlya: mapping on a scale of 1:2,500,000 [O moshchnosti lednikov i kriolitozony Novoi Zemli pri ikh kartirovanii v maßstabe 1:2,500,000]. *Moscow University, Geologica* 33(6), 57–69 (translated by Allerton Press).

Koryakin, V.S. 1986: Decrease in glacier cover on the islands of the Eurasian Arctic during the 20th century [Sokrashcheniye oledeneniya na ostrovakh Yevraziyskoy Arktiki v XX veke]. *Polar Geography and Geology* 10(2), 157–65.

—— 1988: *The glaciers of the Arctic* [Ledniki Arktiki]. Moscow: Nauka, 159 pp. (in Russian).

—— 1997: Glaciers of Novaya Zemlya. *Zemlya i Vselennaya (Earth and Universe)* 1, 17–24 (in Russian).

Kotlyakov, V. and **Kunakhovitch, M.** no date: World Glacier Inventory, National Snow and Ice Data Center, University of Colorado at Boulder, http://www-nsidc. colorado.edu/NOAA/wgms_inventory/asia.html.

Lavrov, M.A. 1932: Notes on the valley glaciers of the Rusanov Valley and Krestovaya Fiord in Novaya Zemlya. Trudy Geologicheskogo Instituta 1, 95–132 (in Russian with English summary).

Livingstone D.M. 1999: Ice break-up on southern Lake Baikal and its relationship to local and regional air temperatures in Siberia and to the North Atlantic Oscillation. *Limnology and Oceanography* 44(6), 1486–97.

Loeng, H. 1991: Features of the physical oceanographic conditions of the Barents Sea. *Polar Research* 10(1), 5–18.

Lubinski, D.J., Forman, S.L. and **Miller, G.H.** 1999: Holocene glacier and climate fluctuations on Franz Josef Land, Arctic Russia, 80°N. *Quaternary Science Reviews* 18, 85–108.

Marshall, J., Kushnir, Y., Chang, P., Hurrell, J., McCartney, M., and **Visbeck, M.** 1997: Atlantic climate variability. 'White paper': http://geoid.mit.edu/accp/avehtml.html.

Matthews, J.A. 1991: The late Neoglacial ('Little Ice Age') glacier maximum in southern Norway: new ^{14}C-dating evidence and climatic implications. *The Holocene* 1, 219–33.

Matzko, J.R. 1993: Physical environment of the underground nuclear test site on Novaya Zemlya, Russia. *USGS Open-file report* 93–501, 28 pp.

Mikhaliov, V.I. and **Chizov, O.P.** 1970: Scientific results of the glaciological investigations on Novaya Zemlya in 1969 [Rezul'taty gliatsiologicheskikh issledovanii na Novoi Zemle v 1969 g]. *Data glaciological studies* 17, 186–99 (in Russian).

Miller, G.H. and **De Vernal, A.** 1992: Will greenhouse warming lead to Northern Hemisphere ice-sheet growth? *Nature* 355, 244–46.

Nesje, A., Johannessen, T. and **Birks, H.J.B.** 1995. Buksdalsbreen, western Norway: climatic effects on the terminal response of a temperate glacier between AD 1901 and 1994. *The Holocene* 5, 343–47.

Overpeck, J. and 17 others 1997: Arctic environmental change of the last four centuries. *Science* 278, 1251–56.

Petermann, A. 1872: Die neuen Norwegischen Aufnahmen des nordostlichen Theiles von Nowaja Semlja durch Mack, Dörma, Carlsen u. A. 1871. *Petermanns Geographische Mitteilungen* 10, 395–96.

Pfirman, S.L., Bauch, D. and **Gammelsrød, T.** 1994: The Northern Barents Sea: water mass distribution and modification. In *The Polar oceans*

and their role in shaping the global environment, Geophysical Monograph 85.

Pohjola, V.A. and **Rogers, J.C.** 1997: Atmospheric circulation and variations in Scandinavian glacier mass balance. *Quaternary Research* 47, 29–36.

Rees, W.G., Dowdeswell, J.A. and **Diament, A.D.** 1995. Analysis of ERS-1 synthetic aperture radar data from Nordaustlandet, Svalbard. *International Journal of Remote Sensing* 16, 905–24.

Rodwell, M.J., Rowell, D.P. and **Folland, C.K.** 1999: Oceanic forcing of the wintertime North Atlantic Oscillation and European climate. *Nature* 398, 320–23.

Rogers, J.C. and **Mosely-Thompson, E.** 1995: Atlantic Arctic cyclones and the mild Siberian winters of the 1980s. *Geophysical Research Letters* 22, 799–802.

Rusanov, V.A. 1910: Areas of fossil ice in Novaya Zemlya. *Comptes Rendus* 150, 807–809 (in French).

—— 1921: The oscillations of shore lines and the retreat of glaciers in Novaya Zemlya. *Revue de Géographie* 9(6), 1–19 (in French).

Shindell, D.T., Miller, R.L., Schmidt, G.A. and **Pandolfo, L.** 1999: Simulation of recent northern winter climate trends by greenhouse-gas forcing. *Nature* 399, 452–55.

Smith, L.C., Forster, R.R., Isacks, B.L. and **Hall, D.K.** 1997: Seasonal climatic forcing of alpine glaciers revealed with orbital synthetic aperture radar. *Journal of Glaciology* 43, 480–88.

Spangler, W.M.L. and **Jenne, R.L.** 1990: World monthly surface station climatology. *National Center for Atmospheric Research Data Report* 2/92.

Stuiver, M. and **Reimer, P.J.** 1993: Extended ^{14}C database and revised CALIB 3.0 ^{14}C calibration program. *Radiocarbon* 35, 215–30.

Svendsen, J.I. and **Mangerud, J.** 1997: Holocene glacial and climatic variations on Spitsbergen, Svalbard. *The Holocene* 7, 45–57.

Thompson, D.W.J. and **Wallace, J.M.** 1998: The Arctic Oscillation signature in the wintertime geopotential height and temperature fields. *Geophysical Research Letters* 25, 1297–300.

Vaganov, E.A., Hughes, M.K., Kirdyanov, A.V., Schweingruber, F.H. and **Silkin, P.P.** 1999: Influence of snowfall and melt timing on tree growth in subarctic Eurasia. *Nature* 400, 149–51.

Warren, C.R. 1993: Rapid recent fluctuations of the calving San Rafael Glacier, Chilean Patagonia: climatic or non-climatic? *Geografiska Annaler* 75A, 111–24.

Warren, C.R. and **Glasser, N.F.** 1992: Contrasting response of south Greenland glaciers to recent climatic change. *Arctic and Alpine Research* 24(2), 124–32.

Werner, A. 1990: Lichen growth rates for the northwest coast of Spitsbergen, Svalbard. *Arctic and Alpine Research* 22, 129–40.

Wiles, G.C., Calkin, P.E. and **Post, A.** 1995: Glacier fluctuations in the Kenai Fjords, Alaska, USA: an evaluation of controls on iceberg-calving glaciers. *Arctic and Alpine Research* 27, 234–45.

Winkler, S. and **Nesje A.** 1999: Moraine formation at an advancing temperate glacier: Brigsdalsbreen, western Norway. *Geografiska Annaler* 81A, 17–30.

Ådlandsvik, B. and **Loeng, H.** 1991: A study of the climatic system in the Barents Sea. *Polar Research* 10(1), 45–49.

Østrem, G. 1964: Ice-cored moraines in Scandinavia. *Geografiska Annaler* 46, 282–332.

—— 1971: Rock glaciers and ice-cored moraines, a reply to D. Barsch. *Geografiska Annaler* 53A, 207–13.